

# Exploration of COX-Like Activity in Wild-Type gp63 Recombinant Protein from *Leishmania mexicana*; Identification of Orthologous Proteins in Clinically Significant Parasites, and Investigation of Arachidonic Acid Binding Sites

[Verónica-Ivonne Hernández-Ramírez](#) , Audifás-Salvador Matus-Meza , [Norma Oviedo](#) ,  
Marco Antonio Magos-Castro , Carlos Osorio-Trujillo , [Lizbeth Salazar-Villatoro](#) ,  
[Luis Alejandro Constantino-Jonapa](#) , [Patricia Talamás-Rohana](#) \*

Posted Date: 31 July 2024

doi: 10.20944/preprints202407.2496.v1

Keywords: *Acanthamoeba castellanii*; COX-like activity; *Entamoeba* spp; *Leishmania mexicana* gp63; *Naegleria fowleri*; *Trypanosoma cruzi*; orthologous proteins to gp63



Preprints.org is a free multidiscipline platform providing preprint service that is dedicated to making early versions of research outputs permanently available and citable. Preprints posted at Preprints.org appear in Web of Science, Crossref, Google Scholar, Scilit, Europe PMC.

Copyright: This is an open access article distributed under the Creative Commons Attribution License which permits unrestricted use, distribution, and reproduction in any medium, provided the original work is properly cited.

## Article

# Exploration of COX-Like Activity in Wild-Type gp63 Recombinant Protein from *Leishmania mexicana*; Identification of Orthologous Proteins in Clinically Significant Parasites, and Investigation of Arachidonic Acid Binding Sites

Verónica-Ivonne Hernández-Ramírez <sup>1</sup>, Audifás-Salvador Matus-Meza <sup>2</sup>, Norma Oviedo <sup>3</sup>, Marco-Antonio Magos-Castro <sup>4</sup>, Carlos Osorio-Trujillo <sup>1</sup>, Lizbeth Salazar-Villatoro <sup>1</sup>, Luis-Alejandro Constantino-Jonapa <sup>5</sup> and Patricia Talamás-Rohana <sup>1,\*</sup>

<sup>1</sup> Departamento de Infectómica y Patogénesis Molecular, CINVESTAV, Av. IPN No. 2508, Col. San Pedro Zacatenco, México City CP 07360, Mexico; vhernandez@cinvestav.mx (V.-I.H.-R.); clostrujillo2@yahoo.com (C.O.-T.); lsalazar@cinvestav.mx (L.S.-V.)

<sup>2</sup> Department of Pharmaceutical Sciences, College of Pharmacy, University of Nebraska Medical Center, Omaha, NB 69198, USA; audifas.matusmeza@unmc.mx

<sup>3</sup> Unidad de Investigación Médica en Inmunología e Infectología, Centro Médico Nacional La Raza, IMSS, Av. Jacarandas S/N, La Raza, Azcapotzalco, México City CP 02990, Mexico; naoviedoa@yahoo.com.mx

<sup>4</sup> Departamento de Genética y Biología Molecular, CINVESTAV, Av. IPN No. 2508, Col. San Pedro Zacatenco, México City CP 07360, Mexico; marcoantoniomagoscastro@gmail.com

<sup>5</sup> Unidad de Investigación UNAM-INC, División de Investigación, Facultad de Medicina, UNAM, Instituto Nacional de Cardiología Ignacio Chávez, México City CP 14080, Mexico; biologia0712@gmail.com

\* Correspondence: ptr@cinvestav.mx

**Abstract:** Recently, we published that the monoclonal antibody (D12 mAb) recognizes gp63 of *L. mexicana*, it is responsible for COX activity. This D12 mAb exhibited cross-reactivity with *Trypanosoma cruzi*, *Entamoeba histolytica*, *Acanthamoeba castellanii*, and *Naegleria fowleri*. COX activity assays performed in these parasites suggested the potential presence of such enzymatic activity. In our investigation, we confirmed that wild-type recombinant gp63 exhibits COX-like activity, in contrast to a mutated recombinant gp63 variant. Consequently, our objective was to identify sequences orthologous to gp63 and subsequently analyze the binding of arachidonic acid (AA) to the putative active sites of these proteins. Given the absence of a crystallized structure for this protein in the Protein Data Bank (PDB), it was imperative to first obtain a three-dimensional structure by homology modeling, using leishmanolysin (PDB ID: LML1) as a template in the Swiss model. Database. The results obtained through molecular docking simulations revealed the primary interactions of AA close to the Zinc atom present in the catalytic site of gp63-like molecules of several parasites, predominantly mediated by hydrogen bonds with HIS264, HIS268 and HIS334. Furthermore, COX activity was evaluated in commensal species such as *E. dispar* and during the encystment process of *E. invadens*.

**Keywords:** *Acanthamoeba castellanii*; COX-like activity; *Entamoeba* spp.; *Leishmania mexicana* gp63; *Naegleria fowleri*; *Trypanosoma cruzi*; orthologous proteins to gp63

## 1. Introduction

Arachidonic acid (AA) is the primary precursor of prostaglandins (PGs) [1]. The release of AA from cellular lipid stores mainly depends on phospholipase A2 [2]. This enzyme hydrolyzes membrane phospholipids, releasing arachidonic acid (AA). Prostaglandin-endoperoxide synthase (PTGS), also known as cyclooxygenases (COX), catalyzes the biosynthesis of prostaglandins and thromboxanes by reducing AA. COX-1 and COX-2, two isoforms of this enzyme, have similar protein structures that catalyze the same reaction [3]. The difference between the two enzymes is that COX-

1 is constitutive; it is part of the homeostatic maintenance of various processes in the human body in most tissues. In comparison, COX-2 is inducible and expressed during inflammatory processes [4].

The COX/PG metabolic axis is one of the most characterized factors in the pathophysiology of host-parasite relationships since it influences the modulation of the immune response. However, the role of the COX/PG axis of parasitic origin during the disease has yet to be thoroughly studied. *E. histolytica* was the first pathogen in which COX-like activity was reported [5].  $\alpha$ -actinin is the protein identified as responsible for COX-like activity in this parasite. Recent reports have documented the role of this amoebic enzyme and PGE2 in the disorganization of the tight junctions of the intestinal epithelium, contributing to the loss of intestinal barrier function and, thus, the occurrence of diarrhea [6]. Recently, our group reported that gp63 from *L. mexicana* (Lmxgp63) is responsible for COX activity [7]. Various molecular factors contribute to the virulence and pathogenicity of *Leishmania* spp. Among these factors, the major surface glycoprotein is highly relevant. Several names have been used interchangeably to describe this glycoprotein. The most used name, gp63, is derived from the 63 kDa glycoprotein, although isoforms with different masses have been found [8]. Leishmanolysin (EC3.4.24.36) was chosen from the IUBMB enzyme nomenclature, reflecting its protease activity. Leishmanolysin belongs to the M8 family of metalloendopeptidases. All M8 metalloproteases contain a zinc-binding HEXXH catalytic site motif [9]. Orthologous surface metallopeptidases exist in both *T. brucei* and *T. cruzi*, although their function differs from that of leishmanolysin [10–12]. Two leishmanolysin homologs are encoded in the *E. histolytica* genome (EhMSP-1 and EhMSP-2), but only one copy of the gene is present in the commensal organism *E. dispar* [13]. Current evidence shows that EhMSP-1 regulates adhesion, motility, destruction of the tissue culture monolayer, and phagocytosis [14].

In recent work a monoclonal antibody (D12) was produced by immunizing mice with fractions enriched with the COX-like activity of *L. mexicana*. Characterization of the antibody showed that D12 recognizes Lmxgp63. Furthermore, immunoprecipitation assays confirmed that Lmxgp63 exhibits COX-like activity in the presence of AA. Cross-antigenicity of this antibody to orthologous gp63 molecules was demonstrated in other parasites using the D12 mAb in confocal microscopy [15]. In this work, we produced recombinant wild type and mutant gp63 proteins from *L. mexicana* and demonstrated that wild type rLmxgp63 protein possesses COX-like activity. Moreover, the presence of RNA transcripts further supports the existence of orthologous proteins in other parasite species. Structural analyses of the COX-2-like antigen revealed continuous and discontinuous epitopes for B cells that could be relevant to explain the cross-reaction of the D12 mAb with different parasites. In addition to the cross-reaction of the D12 mAb, the presence of COX-type activity was confirmed in soluble fractions of *E. histolytica*, the free-living amoebae *N. fowleri* and *A. castellanii* as well as the trypanosomatid *T. cruzi*. For this reason, in the present work, we set out to investigate the possible binding site of arachidonic acid to proteins with possible COX-like activity of the parasite species.

## 2. Materials and Methods

### *Production of a Mutant without COX Activity: Mutation by Frameshift of the gp63 Gene of L. mexicana*

The reading frame of gp63 was shifted in the pPROEX-gp63 vector to obtain a Lmxgp63 protein without COX activity [7]. The histidine tag is linked to the open reading frame (ORF) of the gp63 gene; the NdeI site lies between the histidine tag and the ORF of gp63. The construct, therefore, has a reading frame that is transcribed and translated. Modifications were made in the NdeI restriction site. The plasmid pPROEX-gp63 was cut by the enzyme NdeI and, after that, was purified with phenol-chloroform and precipitated with 1/10 volume 5 M NaCl and 2.5 volumes absolute ethanol. The plasmid was resuspended in 10 mL buffer 2X from the pJET cloning kit (ThermoScientific), plus 7 mL H<sub>2</sub>O and 1 mL DNA blunting enzyme and incubated at 70 °C for 5 min, cooled on ice and mixed with 1  $\mu$ L T4 ligase (5 Weiss units) and 1  $\mu$ L H<sub>2</sub>O. Incubation took place for 30 min at room temperature. Ligations were transformed into *E. coli* DH5<sup>+</sup>, and the plasmid lacking a NdeI site (pPROEX-gp63fs+2 NdeI) was selected by restriction with each enzyme and verified by automated sequencing.

### *Induction and Purification of Recombinant Proteins from Leishmania mexicana gp63*

*E. coli* DH5 /pPROEX-gp63 (wt) and DH5 /pPROEX-gp63fs+2NdeI (mutant) strains were sampled to obtain 5 mL cultures in LB with ampicillin (100 mg/mL). The cultures were incubated overnight at 37 °C. The next day, a 1:100 dilution was prepared in fresh medium (LB/ampicillin 100 mg/mL) and incubated at 37 °C with constant shaking. IPTG at a final concentration of 1 mM was added until the cultures reached an optical density of 0.5 (OD 600 nm). Cultures were stimulated to produce recombinant proteins for 2 h at 37 °C. At the end, cultures were centrifuged at 3,500  $\times g$  for 10 min at 4 °C, and supernatants were removed. The pellets resuspended in 300  $\mu$ L of lysis buffer (10 mM Tris-HCl, pH 7.5, 2 mM EDTA, 0.5 mg/mL Leupeptine, 3 mM N-ethylmaleimide (NEM), 0.5 mg/mL Aprotinin and 1 mM Benzamidine). The pellets were sonicated (10 cycles, 30 seconds of sonication, and 30 seconds of rest at 4 °C). The lysates were centrifuged at 12,000 $\times g$  for 10 min at 4 °C, containing a soluble fraction (SN) and pellet fraction (P). An aliquot of each sample was resuspended in 4X sample buffer for analysis on SDS-PAGE 10 %. A replicate of this material was processed for Western blot analysis. The membrane was blocked and incubated with a commercially available His-Tag Antibody (dilution 1:1000) (HIS.H8, Santa Cruz Biotechnology Cat # sc-57598). The membrane was incubated overnight at 4 °C. Finally, the membrane was washed extensively with TBST and after 1 h incubation at room temperature with the primary antibody, recombinant proteins (rLmxgp63 wild type or rLmxgp63fs+2NdeI mutant) were detected with a secondary anti-mouse IgG HRP antibody (1:1000, Thermo Fisher Cat # 31430). Development was performed by chemiluminescence using the Perkin-Elmer kit using a Newton 7.0 equipment. Because the recombinant proteins were not detected in the supernatants, the pellets were treated with 0.5 % Triton-X100 in lysis buffer. Then, the samples were centrifuged at high speed, and the supernatants were collected, after that, the supernatants were incubated in Eppendorf tubes with Ni-coupled resin (500 mL/100  $\mu$ L). The tubes were gently shaken overnight at 4 °C. The next day, they were centrifuged for 20 s at 4 °C and 1,000  $\times g$ , and the supernatants were removed. The pellets were washed with 500 mL of wash buffer 1 (50 mM Tris-HCl, pH 7.0, 10 mM NaCl and 10 mM imidazole) and then with 500 mL of wash buffer 2 (50 mM Tris-HCl pH 7.0, 10 mM NaCl and 20 mM of imidazole). The pellets were resuspended in elution buffer (50 mM Tris-HCl pH 7, 10 mM NaCl, and 300 mM imidazole). Finally, a pool of eluates was made according to their origin, and they were dialyzed with 50 mM Tris-HCl pH 7.0, 10 mM NaCl, and 30% glycerol for one day at 4 °C, with three changes to a final volume of 2 L dialysis buffer. Samples were then stored at -70°C until use in COX activity assays. In the case of the Western blot, an aliquot of the two eluates obtained from the affinity columns corresponding to the wild recombinant protein or the mutated recombinant protein was used.

### *Parasites*

*Leishmania mexicana* (MHO-M/MX/92/UAY68) promastigote cultures were grown according to works previous [7]. The trophozoites of *Acanthamoeba castellanii*, *Entamoeba dispar*, *Entamoeba invadens*, and *Naegleria fowleri* were donated by Dr. Bibiana Chávez-Munguía. Promastigotes of *Trypanosoma cruzi* were donated by Biol. Lidia Baylon. *Entamoeba histolytica* was cultured according to methods previously documented [16].

### *Obtaining Soluble Fractions from Membrane Components of Various Parasites*

Trophozoites were collected at the end of the logarithmic growth phase by centrifugation for 10 min at 1,500  $\times g$  and 4 °C. In the case of cysts, cells were centrifuged at 3,500  $\times g$  / 7 min. After that, the collected cells were then processed for 8-10 cycles for 1 min each, at full power in a 100-watt ultrasonic processor sonicator in lysis buffer (10 mM Tris-HCl pH 7.5, 2 mM EDTA, 0.5 mg / mL Leupeptin, 3 mM NEM, 0.5 mg / mL Aprotinin and 1 mM Benzamidine). Complete lysis of the parasites was demonstrated under the microscope. The total extracts were centrifuged at 10,000  $\times g$ , the supernatants separated, and the pellets resuspended in 1% Nonidet P-40 in the same lysis buffer. The lysates were centrifuged for 30 min at 10,000  $\times g$  and 4 °C. The resulting supernatant was



separated, aliquoted, and stored at -70 °C until use. Protein concentration was determined using a BCA protein assay (Bio-Rad, Laboraories Inc. DC™ Protein Assay Kit II #5000112).

#### COX Activity

The samples were analyzed according to the method described previously [7]. Briefly, from supernatants obtained from *E. coli* DH5 /pPROEX-gp63 (wt) and DH5 /pPROEX-gp63fs+2NdeI (mutant) with lysis buffer/ 0.5% Triton X-100; as well as soluble fractions obtained from trophozoites of the genus *Entamoeba* and cysts of *E. invadens*, the cyclooxygenase (COX) activity was determined using the COX activity kit (Cat. No. 907-003), Enzo Life Sciences, Inc. Farmingdale, New York, USA). The kit uses a specific chemiluminescent substrate to detect the peroxidative activity of the COX enzyme. COX activity is measured by adding AA. The reaction was read on a Fluoroskan Ascent FL Thermo Labsystem.

#### In Vitro Encystation and Fluorescence Microscopy

*E. invadens* trophozoites of strain IP-1 were cultured according to previous reports [16]. Trophozoites were collected in the logarithmic growth phase ( $5 \times 10^5$ /ml) and transferred to the encystation medium to trigger encystation. Trophozoites, round precysts (20-40 µm), and cysts (10-20 µm) were counted at 24, 48, and 72 h post-induction. Encystation kinetics samples were fixed with 4 % paraformaldehyde for 1 h at room temperature (RT). After three washes with PBS, cells were treated with 10 % bovine serum in PBS for 1 h at 37 °C. Cysts were incubated with 0.01% Calcofluor White M2R (Sigma Chemical, St. Louis, MO) for 60 min at room temperature. This fluorescent dye has a specific affinity for polysaccharides such as chitin. Samples were washed three times with PBS, mounted with Vecta Shield (Vector Laboratories), and observed in a Carl Zeiss LSM 700 confocal microscope. Other samples were treated for immunodetection of gp63. Briefly, cysts were washed three times with PBS and resuspended in 100 µL of PBS; 48 and 72 h samples were subjected to 3 freeze/thaw cycles with N<sub>2</sub> to disrupt the cyst wall. The sample was then treated with 0.5% Triton for 20 min and blocked with 10% fetal bovine serum in PBS for 1 h. Samples were incubated overnight with α-gp63 antibody (CEDARLANE Laboratories Limited, Cat. No. CLP005A, Burlington, Ontario, California) at a 1:50 dilution at 4 °C. The cysts were washed five times with PBS and then incubated for 1 h with the secondary antibody (1:100 dilution of anti-mouse IgG, Alexa Fluor™ 488, Invitrogen), and 1:500 dilution of Hoescht (Chemcruz, Cat. # 33258). After five washes with PBS, the samples were mounted with Vecta Shield (Vector Laboratories) and observed in a Carl Zeiss LSM 700 confocal microscope.

#### Bioinformatics' Analysis

##### Bioinformatic Analyses of Local Alignment Search

The search for proteins homologous to the Lmxgp63 in different parasite species and the analyses of the percentage of identity between these sequences were performed using the BLAST program (<https://blast.ncbi.nlm.nih.gov/Blast.cgi>) [17].

##### Data analysis from RNA-Seq Repositories

Using the Genbank ID or Uniprot ID of gp63 sequences of *Entamoeba*, *Trypanosoma*, *Leishmania*, *Naegleria*, and *Acanthamoeba*, we search the sequence in AmoebaDB ([amoebadb.org](http://amoebadb.org)) and TriTrypDB (<https://tritrypdb.org>).

##### Search in the Gene Ontology Database

The Gene Ontology Term (GOTerm) information was used to identify predicted functions of each sequence of putative gp63 proteins in each species. We also searched for transcript information for each sequence that could indicate a possible role in the life cycle or pathogenesis if available in the database.

## Multiple Alignments

Multiple alignments of the studied sequences were performed using the bioinformatic tool Clustal Omega (<https://www.ebi.ac.uk/Tools/msa/clustalo/>) [18].

## Conserved Domains

The research of conserved domains in the group of proteins similar to *L. mexicana* gp63 and human and mouse COX2 was carried out using the Pfam database (<http://pfam.xfam.org/>) [19].

## Phylogenetic Tree

The phylogenetic tree was constructed using the Neighbor-Joining (NJ) method with a bootstrap of 1000 in MEGAX (<https://www.megasoftware.net/>) [20].

## *Comparative Analysis of the Three-Dimensional Structures of L. mexicana gp63 and Proteins with COX-like Activity from Different Protozoan Parasites*

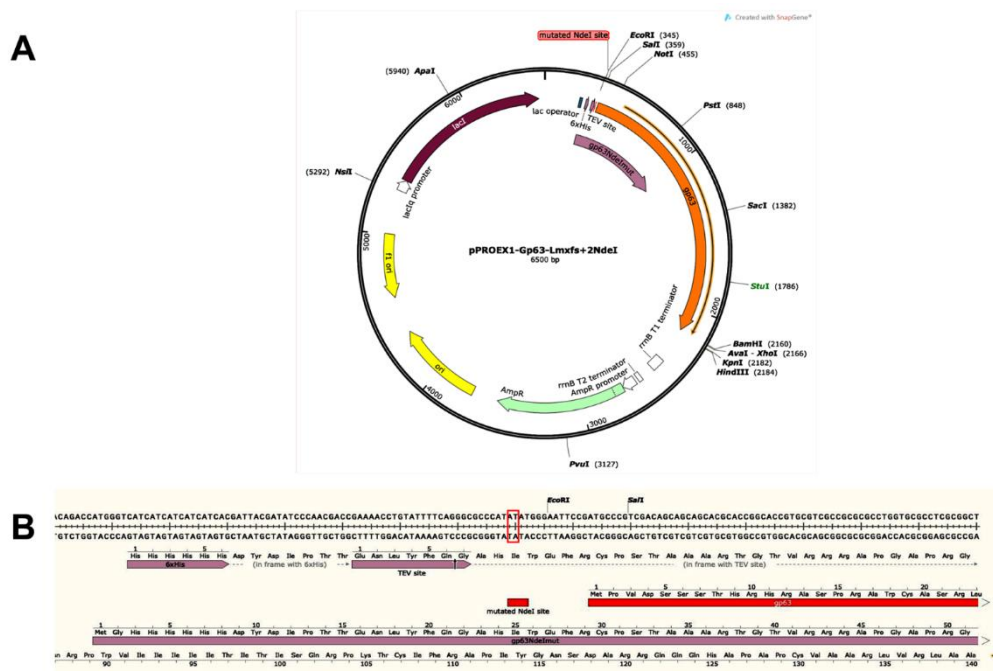
To obtain these structures, all our analyzes were based on the 3D structure of Leishmanolysin from *L. major* (PDB ID: 1LML) since it is the only crystallized structure of Leishmanolysin (gp63) available in databases. Therefore, the three-dimensional structure of Lmxgp63 and the six orthologous proteins were constructed by homology modeling using *L. major* leishmanolysin (PDB ID: 1LML) as a template with Swiss-Model (<https://swissmodel.expasy.org/>) [21]. Then, the alignment and superimposition of the three-dimensional structures obtained were performed using the TopMatch web service (<https://topmatch.services.came.sbg.ac.at/>) [22].

## *Comparative Analysis of the Amino Acid Sequences of the Proteins with COX-like Activity Bound to the AA Structure*

Once again, the new structures were created by homology through the Swiss Model Server. Leishmanolysin (gp63) from *L. major* (PDB ID: 1LML) was used as a template to obtain the structures of *L. mexicana*, *T. cruzi*, *E. histolytica*, *E. dispar*, *E. invadens*, *A. castellanii* and *N. fowleri*. The sequences were obtained from Uniprot with entry numbers Q4DTV2, C4M655, B0ERK0, A0A0A1TW87, L8GQS8, and A0A6A5C651, respectively. Since gp63 is a zinc-dependent metalloprotease, zinc was added to the catalytic site, which was identified by the three histidine residues conserved in all our studied proteins. A similar study with *L. major* was carried out by Mercado-Camarrigo et al. [23]. Energy minimization of each structure was performed using the Yasara server (<http://www.yasara.org/minimizationserver.htm>), and the structures were used for molecular docking. Both the targets and the ligand (AA) in pdb format were uploaded to the SwissDock server (<http://www.swissdock.ch/docking>) for molecular docking. The algorithm involves generating multiple binding modes, evaluating binding energies between the target and ligand using a CHARMM-based scoring function, and selecting and clustering the lowest energy. All obtained predictions were selected for the lowest energy (i.e., the most negative value, the Gibbs free energy,  $\Delta G$ ) and then visualized and analyzed using the UCSF chimera package v.1.15 [24].

## Statistical Analysis

All tests were performed in three independent replicates. A one-way ANOVA with the Tukey Post hoc test determined statistical differences between groups. All analyses were made in Graph Pad Prism V 8.0.2.



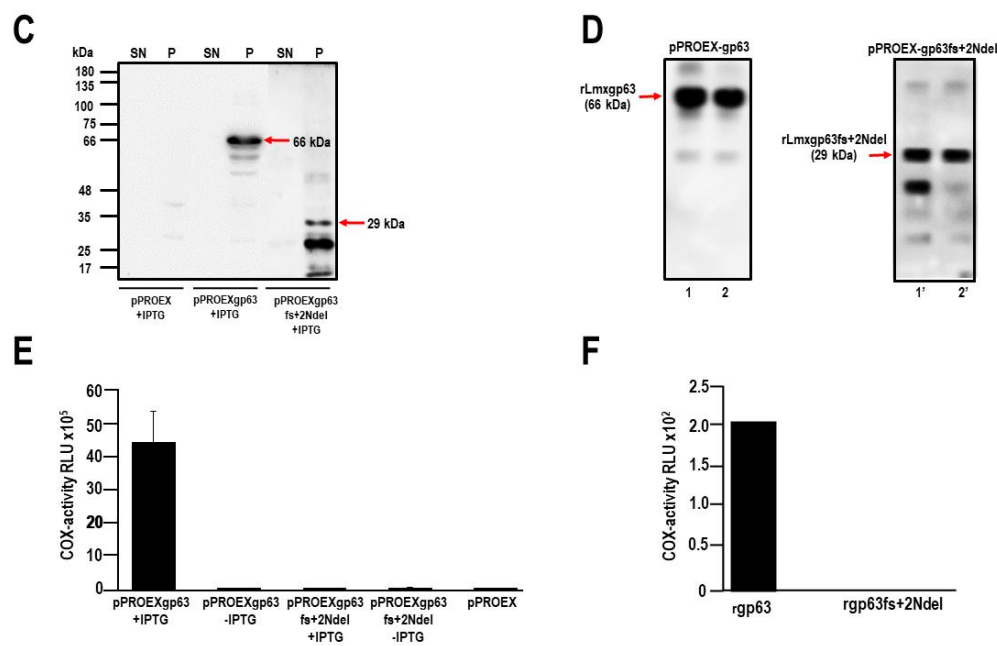


**Figure 1.** Role of the *L. mexicana* gp63 protein in COX-like activity. (A) The plasmid map highlights a mutated *NdeI* site in the *L. mexicana* His-tag-gp63 protein, with a new peptide indicated by a pink arrow produced by a different reading frame. (B) Changes in the *NdeI* site's reading frame in amino acids are shown for both wild type and mutant proteins. The red box signifies the insertion of two nucleotides, resulting in a 262 amino acid product with a molecular weight of 29 kDa. (C) Western blot analysis of proteins from *E. coli* DH5α transformed with wild type (pPROEX-gp63) and mutant (pPROEX-gp63fs+2Ndel) plasmids on a 10% SDS-PAGE gel. Plasmid pPROEX served as a control. Recombinant gp63 proteins were detected using a commercial anti-tag histidine antibody (1:1000) in the presence of IPTG. Supernatant = SN; Pellet = P. (D) Recombinant protein purification from Triton-X100 solubilized pellets of rpLmxPROEX-gp63 and rpLmxPROEX-gp63fs+2Ndel transformed bacteria, followed by Ni<sup>2+</sup> resin incubation and analysis via 15 % SDS-PAGE and Western blot. Lanes 1 and 2 correspond to two eluates of the protein, wild recombinant, and in 1' and 2' two eluates corresponding to the mutant recombinant protein are shown. (E) Assessment of COX-like activity in wild type and mutant constructs' total extracts using a COX activity kit, with the vector serving as a negative control. These experiments were done in triplicate conducted in three independently performed biological assays. Purified recombinant proteins were concentrated and subjected to dialysis with renaturation buffer. (F) COX activity detected in purified recombinant proteins, with analyses conducted in triplicate across two independent experiments.

3.2. *Trypanosoma cruzi*, *Entamoeba histolytica*, *Entamoeba dispar*, *Entamoeba invadens*, *Acanthamoeba castellanii* and *Naegleria fowleri* Contain Proteins Orthologous to gp63 of *L. mexicana*

3.2.1. Bioformatic analysis for the identification of orthologous proteins.

We have already mentioned in previous work that several parasites exhibit COX activity [15]. As the monoclonal antibody D12 is directed against Lmxgp63 and cross-reacts with other proteins from different species, the presence of conserved discontinuous epitopes presents in each of the gp63 analyzed in this study (*T. cruzi*, *E. histolytica*, *A. castellanii*, and *N. fowleri*) was established [15]. Lmxgp63 is a zinc-dependent metalloprotease and is considered a molecular factor contributing to the virulence and pathogenesis of *Leishmania* parasites. This protease is also called MSP, PSP, or leishmanolysin [25]. Therefore, the next approach was to perform a bioinformatic analysis to look for the presence of orthologues proteins to Lmxgp63 in the different parasites included in this study. To carry out a preliminary search for similarity between proteins from various parasites with Lmxgp63, a local alignment bioinformatic analysis (BLAST) was performed. Table 1 shows the identified



orthologous proteins to gp63 in the different parasites. Two other species of the genus *Entamoeba*, *E. dispar*, which has reduced virulence properties, as well as *E. invadens*, since it is the only species that can form cysts *in vitro*, were also included. The identity percentage of the *L. mexicana* gp63 and the different sequences varies between 37.86% and 25.81%. The highest percentage of identity was found for *T. cruzi* (XP\_817808.1) and the lowest percentage for *E. dispar* (XP001740726.1). In the case of *E. invadens*, *E. dispar*, and *N. fowleri*, the proteins are considered hypothetical proteins; those of *T. cruzi* and *E. histolytica* are gp63 cell surface proteases; and *A. castellanii* gp63 is a putative leishmanolysin.

**Table 1.** A BLAST search for sequences like *L. mexicana* gp63 in different parasitic protozoa.

Description	Query cover	E value	% Identity	%	Accession
<i>Leishmania mexicana</i> (GP63, leishmanolysin)	0.0	100	100		XP_003872886.1
<i>Trypanosoma cruzi</i> (surface protease GP63)	2e <sup>-111</sup>	86	37.86		XP_817808.1
<i>Entamoeba histolytica</i> (surface protease GP63)	1e <sup>-36</sup>	71	27.43		XP_652632.1
<i>Entamoeba dispar</i> (hypothetical protein)	1e <sup>-34</sup>	81	25.81		XP_001740726.1
<i>Entamoeba invadens</i> (hypothetical protein)	1e <sup>-31</sup>	66	27.59		XP_004184102.1
<i>Acanthamoeba castellanii</i> (leishmanolysin, putative)	1e <sup>-45</sup>	52	32.75		XP_004337275.1
<i>Naegleria fowleri</i> (hypothetical protein)	1e <sup>-29</sup>	52	28.24		KAF0981298.1

Hypothetical proteins are proteins predicted from nucleic acid sequences and whose existence has not been proven. In the case of identified putative proteins in the genome, there is no evidence of the function of these proteins. In both cases it was decided to perform a BLAST transcript analysis of these proteins in RNA-seq groups of the different parasites analyzed. Figure 2 shows that except for *A. castellanii*, it was not possible to detect the existence of mRNA for the putative leishmanolysin proteins identified by BLAST. Previously, we reported that the D12 mAb recognizes epitopes on *A. castellanii* and *N. fowleri* trophozoites, and this antibody has been shown to recognize discontinuous epitopes from *L. mexicana* gp63 [15]. These results indicate the existence of orthologous proteins of the various parasites analyzed, to gp63 of *L. mexicana*.

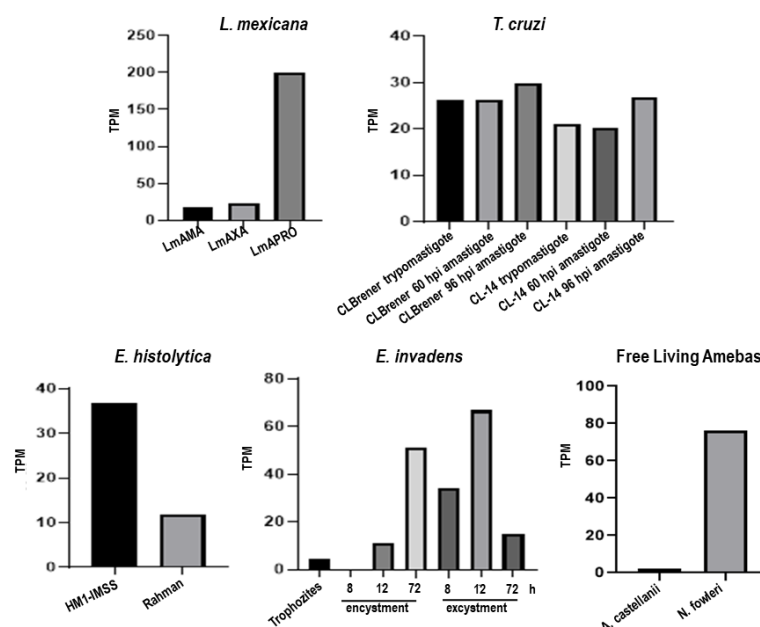


**Figure 2.** Analysis of RNA-seq data repositories from various parasites including *L. mexicana*, *T. cruzi*, *E. histolytica*, *E. dispar*, *E. invadens*, *A. castellanii*, and *N. fowleri*. The figure illustrates the presence of transcripts per million (TPM) of mRNA corresponding to the gp63 protein in *L. mexicana* and orthologous proteins in the analyzed parasites. The TPM value indicates a relative expression level across the samples. Data for this analysis were from AmoebaDB and TriTrypDB (<https://tritrypdb.org>).

Therefore, to establish a possible functional relationship between orthologous proteins with gp63, a multiple alignment was performed. Figure 3A shows the alignment of the protein sequences of each parasite. The catalytic site region is indicated on a purple background, and the HExxHAXGF motif, which is conserved across the 7 proteins analyzed, can be seen. The sequences of the candidate proteins were examined using the Pfam database to determine the presence of functional domains like the *L. mexicana* gp63 (Figure 3B). The results confirmed that all analyzed sequences share the same domain of the M8 peptidase family. This domain was reported to be present in *L. mexicana* gp63 [25]. This enzyme is found in eukaryotes, including *Leishmania* and other protozoan parasites. A domain of the Transcription Factor Immunoglobulin (TIG) family, called IPT/TIG, was identified in the *E. histolytica* protein. This domain is characterized by a fold like that of immunoglobulin and is found in tyrosine kinase receptors such as Met and Ron receptors. In addition, this domain is also present in transcription factors involved in DNA binding [26] (Figure 3B).

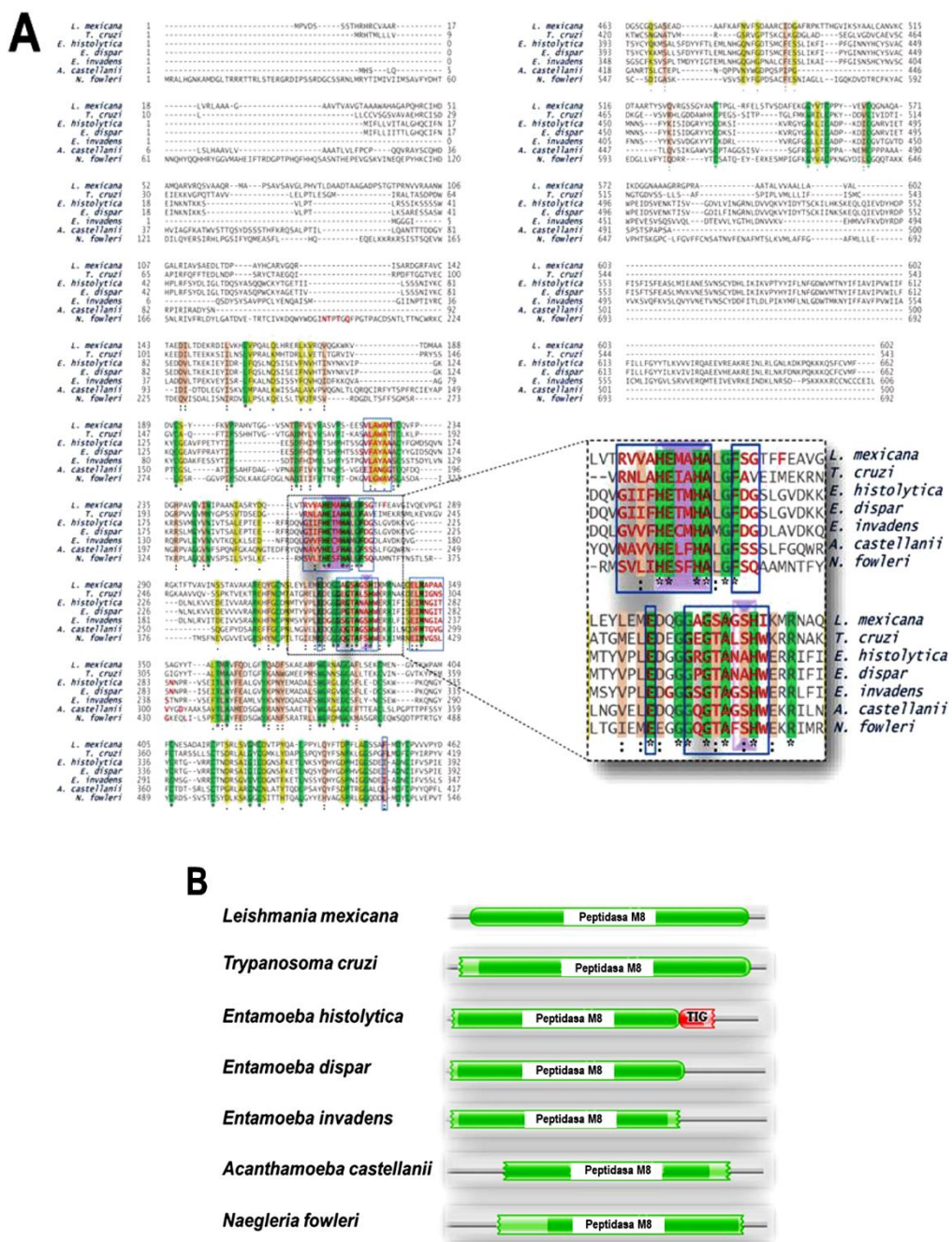


**Figure 3.** (A) Multiple sequence alignments of proteins like the *L. mexicana* gp63 protein (XP\_003872886.1) alongside counterparts from *T. cruzi* (XP\_817808.1), *E. histolytica* (XP\_652632.1), *E.*

*dispar* (XP\_001740726.1), *E. invadens* (XP\_004184102.1), *A. castellanii* (XP\_004337275.1), and *N. fowleri* (KAF0981298.1). The alignment, generated using Clustal Omega, highlights highly conserved or identical residues in red. Green shading indicates identical residues, while light brown and yellow denote moderately and low conserved residues, respectively. Red letters within blue boxes represent regions within 10 Å of the zinc atom, while purple background highlights the catalytic site. (B) Conserved domains in proteins homologous to gp63. All examined proteins contain the leishmanolysin domain, belonging to the M8 peptidase family, spanning specific regions: 46–570 in *L. mexicana*, 58–510 in *T. cruzi*, 27–490 in *E. histolytica*, 28–490 in *E. dispar*, 32–423 in *E. invadens*, 103–406 in *A. castellanii*, and 222–632 in *N. fowleri*.

A phylogenetic tree was constructed to infer the evolutionary history of the studied proteins, using the gp63 protein from *L. mexicana* and the orthologous proteins of the six protozoa species. Figure 4 shows an ancestral relationship between the sequences of *L. mexicana* and the proteins orthologous to gp63 of *T. cruzi*; thus, these two taxa are the most closely related. The next closest related taxon is *A. castellanii*, which shares an internal node with the mentioned taxa. Concerning the genus *Entamoeba*, the COX-like activity sequence of *E. histolytica* is preferentially linked to a node within *A. castellanii*. Finally, the *N. fowleri* sequence is phylogenetically related to an internal node of *A. castellanii*.

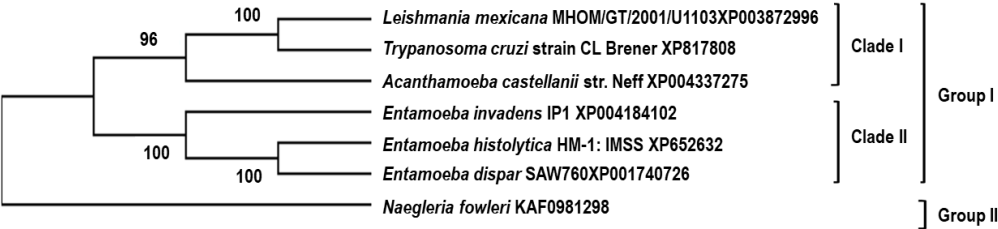


**Figure 4.** A phylogenetic tree was constructed for proteins similar to gp63 from *L. mexicana*. The tree was generated using the complete amino acid sequences of the studied proteins via the neighbor-joining method, employing the phylogenetic inference package (PHYMLIP) version 3.5c. The construction utilized the amino acid sequence of gp63 from *L. mexicana* along with orthologous sequences from various parasites, including *L. mexicana* (XP\_003872886.1), *T. cruzi* (XP\_817808.1), *E. histolytica* (XP\_652632.1), *E. dispar* (XP\_001740726.1), *E. invadens* (XP\_004184102.1), *A. castellanii* (XP\_004337275.1), and *N. fowleri* (KAF0981298.1).

3.3. Orthologous Proteins Have Characteristics of Metalloproteinases

3.3.1. Ontology of Genes Orthologous to gp63 of *L. mexicana*

In addition, the sequences and predicted functions of proteins orthologous to *Leishmania* gp63 were analyzed using AmoebaDB for Amoeba species or TriTrypDB for trypanosomatids. Each sequence used in this work was identified in the database. The primary molecular function identified for each sequence of *E. histolytica*, *T. cruzi*, *L. mexicana*, *E. dispar*, *E. invadens*, *A. castellanii*, and *N. fowleri* was the metalloendopeptidase activity (GOTerm: GO: 0004222). The GOTERM for proteolysis (GO: 0006508) and cell adhesion (GO: 0007155) were also proposed for each sequence. A characteristic feature of metalloproteinase proteins is the need to bind zinc for their enzymatic activity. This function is presented as metal ion binding (GOTERM: GO: 0046872) in both *L. mexicana* and *T. cruzi*; only *E. histolytica* of the amoeba species has the GOTERM for zinc ion binding (GO: 0008270). The GOTERMS assigned for each sequence are listed in Table 2.

**Table 2.** Predicted functions of gp63 homologues in Trypanosomatids and Amoeba species. .

Species	Gene bank ID	Uniprot ID	TriTrypDB/ AmoebaDB	Name of protein	Gene Ontology Predicted functions
<i>L. mexicana</i>	XP_003872886.1	E9AN57	LmxM.10.0470	GP63, leishmnolysin	GO: 0004222 metalloendopeptidase activity GO: 0005886 plasma membrane GO: 0006508 proteolysis GO: 0007155 cell adhesion GO: 0016020 membrane GO: 0046872 metal ion binding
<i>T. cruzi</i>	XP_817808.1	Q4DTV2	TcCLB.508693.100	Surface protease GP63 putative	GO: 0004222 metalloendopeptidase activity GO: 0005886 plasma membrane GO: 0006508 proteolysis GO: 0007155 cell adhesion GO: 0016020 membrane GO: 0046872 metal ion binding
<i>E. histolytica</i>	XP_655632.1	C4M655	EH.042870	Cell surface protease gp63puttive	GO: 0004222 metalloendopeptidase activity GO: 0005886 plasma membrane GO: 0006508 proteolysis GO: 0007155 cell adhesion GO: 0008270 zinc ion binding GO: 0016020 membrane
<i>E. dispar</i>	XP_001740726.1	B0ERK0	EDI_037980	Hypothetical protein conserved	GO: 0004222 metalloendopeptidase activity GO: 0005886 plasma membrane GO: 0006508 proteolysis GO: 0007155 cell adhesion GO: 0016020 membrane GO: 0016021 integral component of membrane
<i>E. invadens</i>	XP_004184102.1	A0A0A1TW87	EIN_174510	Hypothetical protein	GO: 0004222 metalloendopeptidase activity GO: 0006508 proteolysis GO: 0007155 cell adhesion GO: 0016020 membrane GO: 0016021 integral component of membrane
<i>A. castellanii</i>	XP_004337275.1	L8GQS8	ACA1_29880	Leishmanolysin putative	GO: 0004222 metalloendopeptidase activity GO: 0006508 proteolysis GO: 0007155 cell adhesion GO: 0016020 membrane
<i>N. fowleri</i>	KAF09812981	A0A6A5C651	NF0068990	Metalloendopeptidase zinc ion binding protein	GO: 0004222 metalloendopeptidase activity GO: 0006508 proteolysis GO: 0007155 cell adhesion GO: 0016020 membrane

These results suggest that each sequence is a gp63-like protein, although only three of them have gp63 in their name entry: *E. histolytica*, *T. cruzi*, and *L. mexicana*. The others include hypothetical proteins with this name (*E. dispar* and *E. invadens*), a putative leishmanolysin (*A. castellanii*), and a metalloendopeptidase zinc ion binding protein (*N. fowleri*).



### 3.4. The gp63 of *L. mexicana*, and the Orthologous Proteins Present in *T. cruzi*, *Entamoeba histolytica*, *Entamoeba dispar*, *E. invadens*, *A. castellanii*, and *N. fowleri*, Have a Probable Binding Site for Arachidonic Acid

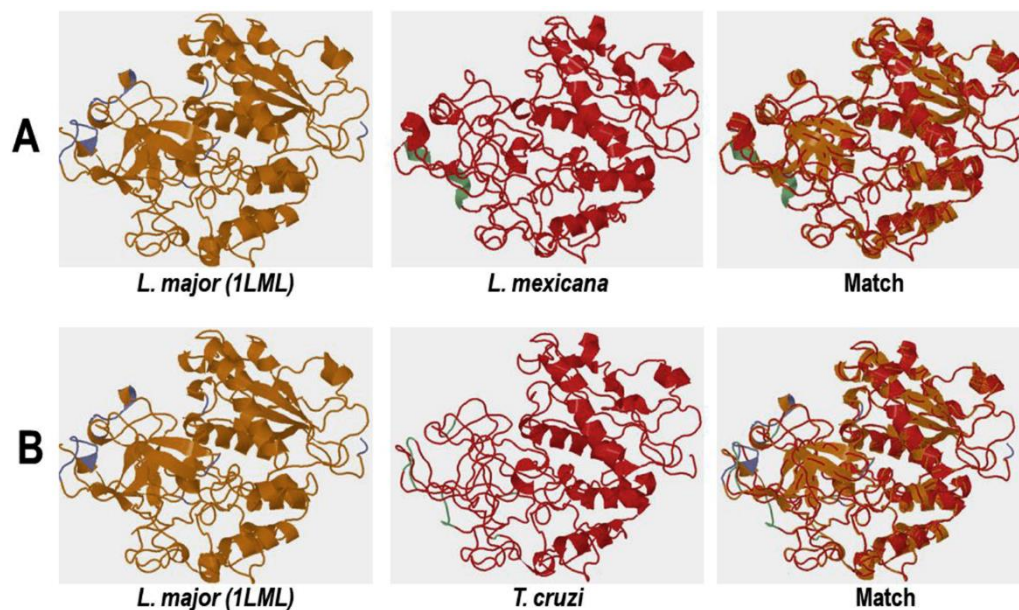
#### 3.4.1. Conformational analysis of gp63

The 3D analysis performed with TopMach-web is a computational tool used to analyze protein structure alignments [22]. Since the crystallized structure of gp63 from *L. mexicana* has yet to be reported, the 3D structure was modeled using the leishmanolysin of *L. major* (PDB ID: 1LML) as a template using SWISS-MODEL. To proceed with the identity analyses between leishmanolysin from *L. major* and *L. mexicana*, the structural similarity between these two molecules was determined. Supplementary figure 1Aa shows the overlay corresponding to the 3D molecules; structurally equivalent parts of the proteins appear in red. The BLAST analysis showed 81.06% of identity between the sequences of *L. major* and *L. mexicana* gp63 proteins, with a coverage of 97% (SF1Ab). Supplementary Figure 1B shows a detailed comparison, both structural (1, 2, and 3 upper panels) and sequences (1', 2', and 3' lower panels), between these two proteins. Similar structures that consist of highly conserved amino acid sequences are shown in white that correspond to the region between residues 109-209 (SF1B 1,1'); the region between residues 419-489 (SF1B 2,2'), and the region between residues 509-569 (SF1B 3,3'). In the three figures, red regions correspond to structures that are similar with low identity, and in green the structures that are not shared.

This result is consistent with data obtained from the analysis of the crystallized structure of PDB ID: 1LML from *L. major* with the leishmanolysin sequence (UniProt ID A0A088RJB7) from *L. panamensis* [23]. Therefore, leishmanolysin of *L. mexicana* is orthologous to gp63 from *L. major*. Then, the proteins of all parasites modeled in SWISS-MODEL were included in this analysis.

Having established the identity between Leishmanolysin of *L. major* and gp63 of *L. mexicana*, it was decided to analyze the 3D structure of the orthologous proteins using Leishmanolysin of *L. major* (PDB ID: 1LML) as a template.

Figure 5A shows the 3D structural models of *L. major* Leishmanolysin (left panel) and *L. mexicana* gp63 (middle panel) and their overlay (Match). As shown in the matchboxes, the structures observed in orange and red correspond to the structurally aligned residues, with the structure shown in orange representing the query protein and those in red representing the target protein. Structures in green or blue correspond to unaligned residues of the query and target proteins, respectively. A high similarity was also observed when the same analysis was performed, now between *L. major* leishmanolysin and orthologous protein of *T. cruzi* (Figure 5B) of *Entamoeba* sp. (Figure 5C), and free-living amoebae (Figure 5D).



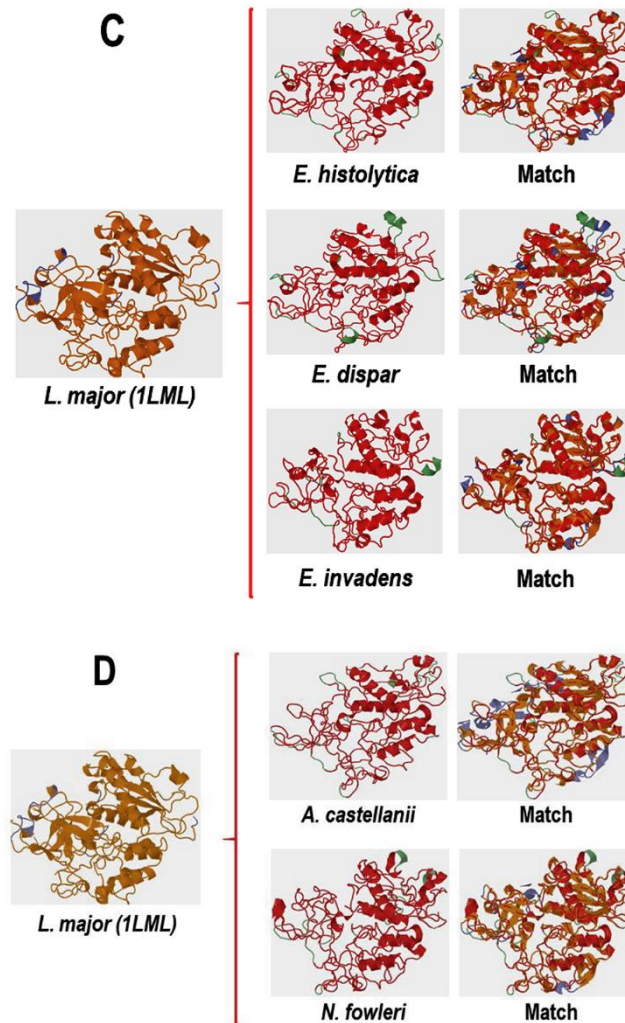


**Figure 5.** Comparing the three-dimensional structures of proteins orthologous to *L. mexicana* gp63: The 3D structures of the analyzed proteins were modeled using SWISS-MODEL. Subsequently, the overlap analysis of these structures was conducted using TopMatch-web. In the visual representation, structurally aligned sequences are highlighted in orange and red to indicate a match, while dissimilar structures are depicted in green or blue. (A) Comparative analysis between *L. major* (PDB ID: LML1) and *L. mexicana* (XP\_003872886.1) is illustrated. (B) Comparison between the leishmanolysin (PDB ID: LML1) of *L. major* and protein XP\_817808.1 of *T. cruzi* is shown. (C) Sequences from the genus *Entamoeba* (*E. histolytica* XP\_652632.1, *E. dispar* XP\_001740726, and *E. invadens* XP\_004184102.1) are compared with the leishmanolysin (PDB ID: LML1) from *L. major*. (D) Comparative analysis with free-living amoebae, *A. castellanii* and *N. fowleri* (XP\_004337275.1, NKA0981298.1), respectively, is presented.

The values obtained by the analysis with TopMatch-web show that the analyzed structural models are very similar regarding the structure of *L. major* gp63 since the value of aligned residues (Length) and the measurement of aligned residues (Score) were very similar (Table 3). The root mean square deviation (RMS), which determines the distance of the overlapping residues of aligned structures, was between 0.44 and 0.79. Therefore, these results suggest that the query and target sequences are similar. For the *L. mexicana* gp63 protein, superimposing the three-dimensional structure with the structure of the 1LML protein gives an RMS value of 0.07, as shown in Table 3, since they belong to the same genus. Furthermore, their amino acid sequence alignment showed 81% identity (SI % value, Table 3).

**Table 3.** Values of the superposition of the structure’s analysis. (Length) The number of pairs of residues that are structurally equivalent; (QC %) Query cover based on alignment length, expressed in percent; (TC %) Target cover based on alignment length, expressed in percent; (Score) Measure of structural similarity; (RMS) Root-mean-square error of the superposition in Ångströms; and (SI %) Sequence identity of the query and target in the equivalent regions, expressed in percent.

Description	Length	QC%	TC%	Score	RMS	SI%
<i>Leishmania mexicana</i>	465	100	98	465	0.07	81
<i>Trypanosoma cruzi</i>	444	95	97	442	0.44	39
<i>Entamoeba histolytica</i>	424	91	89	20	.73	25
<i>Entamoeba dispar</i>	405	87	89	400	0.79	26
<i>Entamoeba invadens</i>	418	89	93	414	0.69	20
<i>Acanthamoeba castellanii</i>	377	81	91	373	0.73	31
<i>Naegleria fowleri</i>	432	93	90	428	0.68	28

3.4.2. Molecular Docking Analysis

After confirming the similarity among all the analyzed orthologues proteins with *L. major* leishmanolysin, a molecular docking analysis was performed to analyze the likely binding site for the AA in these structures. Figure 6A shows in the left panel, the 3D structure of leishmanolysin from *L. major* at the bottom and its catalytic site (Figure 6B). The middle panel shows the result of the molecular docking of AA to the different structures of the orthologues to gp63 of *L. mexicana* of the different parasites analyzed. Applying the algorithm used by SwissDock, AA (shown in purple) was found to have a preferential affinity toward the catalytic site in most molecular targets, except for *T. cruzi* and *E. invadens*, where the affinity occurred at a non-catalytic site. Although the amino acids of the histidine triad along with the glutamic acid are present in the motif (HExxHAXGF) (Figure 3A), most likely, the presence of the other amino acid residues in the area surrounding the motif creates a conformation that changes the nature and affinity of the histidine triad catalytic site for AA. The rightmost panel (Figure 6B) shows a close-up of the interaction between the catalytic site and the position occupied by the AA in each protein that maintains their affinity. The three histidine and glutamic acid are observed together with the zinc atom.

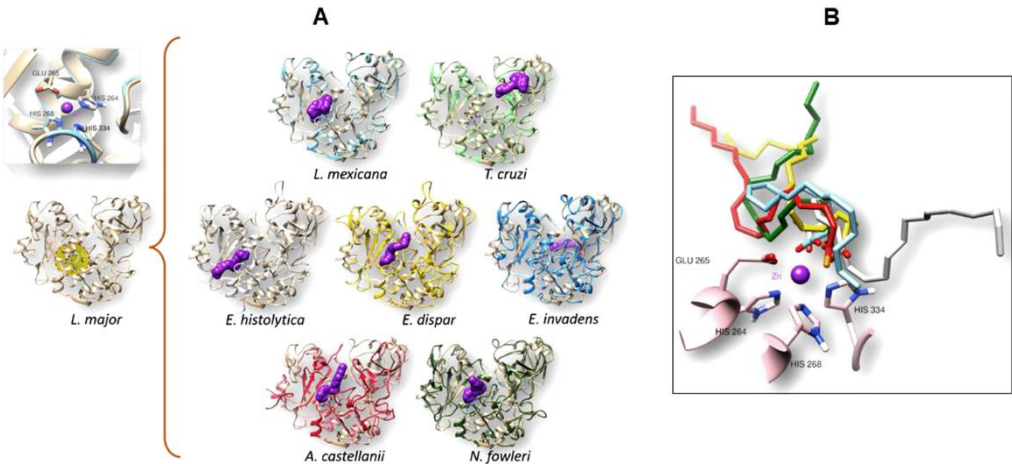


**Figure 6.** Molecular docking between arachidonic acid (AA) and each studied target. (A) Displays overlapping structures of *L. major* with each model obtained by homology modeling. The surface of the ligand is highlighted in purple. (B) Provides an expanded view of the catalytic site of *L. mexicana*, showcasing the superposition of each obtained ligand. The ligands showing affinity for the catalytic site of the molecular docking study are represented as follows: light blue for *L. mexicana*, light green for *T. cruzi*, gray for *E. histolytica*, yellow for *E. dispar*, blue for *E. invadens*, red for *A. castellanii*, and dark green for *N. fowleri*.



We can also observe that each AA (shown in color depending on the protein under study) took a different arrangement due to the high degree of freedom of the polyunsaturated hydrocarbon chain. However, the orientation of the carboxylic acid of the AA molecules is toward the zinc atom, forming hydrogen bonds to histidine. The types of interactions found in the molecular docking of AA to each of the analyzed proteins are described in detail below. Figure 7 shows the interaction of AA with the catalytic site and the interaction of the zinc atom with the carboxylic acid of AA for *L. mexicana*, *E. histolytica*, *E. dispar*, *A. castellanii*, and *N. fowleri* (highlighted images with thick border). It also depicts hydrogen bonding interactions with HIS264, HIS206, and HIS267 for *L. mexicana*, *E. histolytica*, and *E. dispar*, respectively. In the case of *T. cruzi* and *E. invadens*, the AA was in a pocket distant from the catalytic site, and only *T. cruzi* showed hydrogen bonds with ARG416 and TYR379. In both *A. castellanii* and *N. fowleri*, AA also interacted with the catalytic site. However, no hydrogen bonds with histidine residues of the catalytic site were detected with the algorithm used in this study, and the interactions they did show were predominantly hydrophobic.

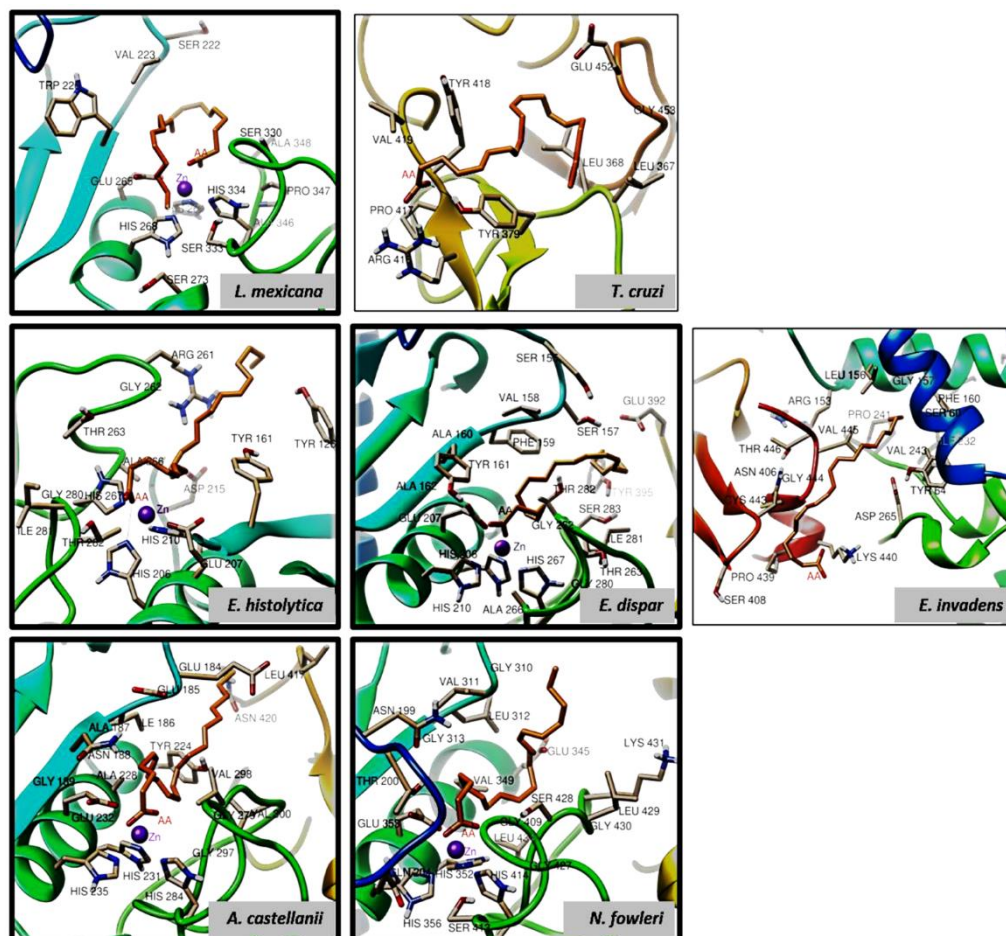


**Figure 7.** The binding modes of arachidonic acid (AA) with targets of each parasite are as follows: *L. mexicana* involves hydrogen bonds with HIS264; *T. cruzi* shows hydrogen bonds with TYR379 and ARG416; *E. histolytica* forms hydrogen bonds with HIS206; *E. dispar* establishes hydrogen bonds with HIS267 and GLU207. For *A. castellanii* and *N. fowleri*, the binding between the gp63-like proteins and AA occurs through hydrophobic bonds. The interaction of the zinc atom with the carboxylic acid of AA is shown in the images with a thick border. .

Likewise, it is important to mention that the binding energy found in both organisms was one of the most favorable (Table 4). Finally, Table 4 summarizes the main observed interactions between AA and the modeled proteins, and the hydrogen positions found. In addition to the triad of histidine residues forming the catalytic site, the presence of glutamic acid was also preserved. Interestingly,



the two modeled proteins from *T. cruzi* and *E. invadens* have less preferred binding energies than those interacting with the catalytic site.

**Table 4.** Binding energies and molecular interactions of AA with targets of each parasite. Histidine and glutamate residues respectively present in the catalytic site are shown in red and blue.

Organism	Interaction residues on the binding site	H-bond	Energy (kcal/mol)
<i>L. mexicana</i>	VAL223 SER222 ALA348 SER330 PRO347 ALA346 HIS334 SER333 SER273 HIS268 GLU265 P.T.-R.226 HIS264	HIS264	-11.16
<i>T. cruzi</i>	GLU452 GLY453 LEU367 LEU368 TYR379 ARG416 PRO417 VAL419 TYR418	TYR379 ARG416	-8.84
<i>E. histolytica</i>	ARG261 TYR161 TYR126 HIS210 GLU207 HIS206 THR282 ILE281 GLY280 HIS267 ALA266 THR263 GLY262 ASP215	HIS206	-9.57
<i>E. dispar</i>	SER155 SER157 GLU392 TYR395 THR282 SER283 ILE281 GLY262 THR263 GLY280 ALA266 HIS267 HIS210 HIS206 GLU207 ALA162 ALA160 TYR161 PHE159 VAL158	HIS267 GLU207	-10.32
<i>E. invadens</i>	LEU156 GLY157 PHE160 SER60 ILE232 VAL243 TYR64 ASP265 LYS440 PRO439 SER408 CYS443 ASN406 THR446 ARG153 PRO241	---	-8.92
<i>A. castellanii</i>	GLU184 LEU417 ASN420 VAL298 VAL300 GLY279 GLY297 HIS284 HIS231 HIS235 GLU232 GLY189 ALA228 ASN188 ALA187 ILE186 GLU185 GLY310 LEU312 GLU345 SER428 LYS431 LEU429 GLY430 GLY409 LEU434 GKY427	---	-11.02
<i>N. fowleri</i>	HIS414 SER413 HIS356 GLN204 HIS352 GLU353 THR200 GLY313 ASN199 VAL311	---	-10.81

3.5. The *Entamoeba* genus Contains a COX-like Activity Which Is Present during the Encystment Process of *E. invadens*

3.5.1. Determination of COX Activity from Soluble Fractions of *E. histolytica*, *E. dispar* and *E. invadens*, Using Exogenous AA and the Commercial COX Activity Kit

The presence of COX-like activity has been reported in the promastigote and amastigote forms of *L. mexicana* [7]. Therefore, the possibility of a COX-like involvement in the life cycle of parasites could be conceivable. In this context, *E. invadens* was included in this study because, under culture conditions, it is possible to maintain the two phases of the cell cycle: the cyst and the trophozoites. Therefore, COX activity was first determined with the commercial kit, using exogenous AA in the supernatants extracted from the different extracts of trophozoites of the genus *Entamoeba*. Figure 8A shows COX-like activity in *E. histolytica*, *E. dispar*, and *E. invadens*. The results obtained show that all species have COX activity. Assays were performed with normalized protein concentration, using a final 50 mg/25 mL concentration when analyzing COX activity. Therefore, we propose that *E. histolytica* exhibits the highest COX activity compared to *E. dispar* and *E. invadens* under these conditions.

3.5.2. Detection of COX Activity during the Encystment of *E. invadens* Trophozoites

After confirming that *E. invadens* has COX activity, we induced encysting trophozoites to purify cysts at various points of the process. Figure 8Ba shows an aliquot of cysts analyzed with calcofluor using confocal microscopy. This compound binds to chitin, a carbohydrate located in the cyst wall (48 h after cyst induction). Figure 4Bb shows the purity of the sample by DIC using confocal

microscopy. A replicate of this material was analyzed, and figure 8C shows the presence of COX activity during encystation kinetics, demonstrating a maximum activity at 48 h post-induction. In addition, immunofluorescence analysis was performed during the encystment process of *E. invadens*, using the commercial monoclonal antibody anti-gp63 from *L. major*. Although cross reaction with this antibody occurs early after induction of encystation (24 h), figure 8D shows the cross-reaction after 48 h after of encystment (Figure 8Da), when the highest amount of the antigen was detected. At 24 h, only a few cells were recognized by the antibody. The recognition pattern remained until 72 h (data not shown), strongly suggesting the presence of gp63 in cysts. DIC was used to confirm the purification process of the cysts (Figure 8Db).

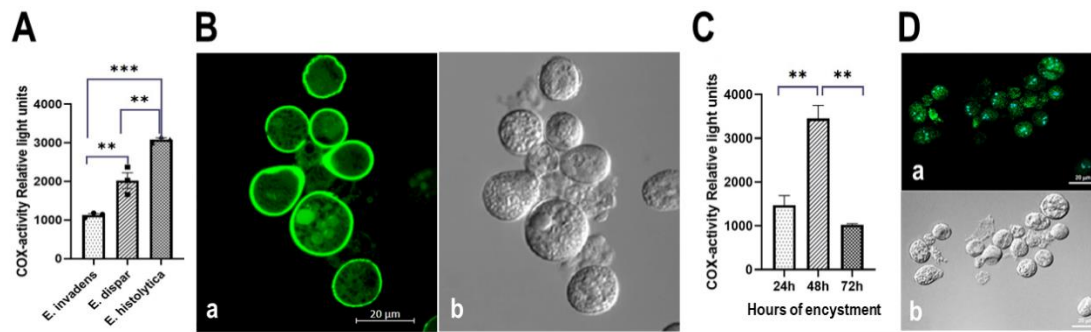


**Figure 8.** *E. histolytica*, *E. dispar*, and *E. invadens* exhibit COX-like activity. A) COX activity detection in the genus *Entamoeba* involved using a commercial kit and exogenous AA in soluble fractions (50  $\mu$ g protein/25  $\mu$ L). B-D) Presence of COX-type activity during the encystation process: In (Ba), cyst presence was confirmed by calcofluor staining, with cyst purity validated through DIC microscopy analysis (Bb). This sample represents the 48-hour encystment process. COX-type activity determination during encystment utilized the commercial kit and exogenous A.A., with trophozoite and cyst extracts' soluble fractions tested using exogenous AA at a final concentration of 20  $\mu$ M (C). In (Da), gp63 presence in 48-hour-induced cysts was observed using anti-*Leishmania major* gp63 monoclonal antibody (CEDARLANE Laboratories Limited, Cat. No. CLP005A, Burlington, Ontario, CA), with the reaction developed through incubation with anti-mouse IgG coupled to FITC. Sample purity was analyzed through DIC microscopy (Db). Three independent biological replicates were conducted in triplicate.

#### 4. Discussion

Eicosanoids are active lipid products often derived from arachidonic acid (AA). They are produced primarily via several enzymatic pathways, including cyclooxygenases (COX), lipoxygenases (LOX), and cytochrome P-450 epoxygenase (CYP450). Alternatively, a small proportion of eicosanoids are formed by autoxidation of AA [27]. In recent years, research has focused on the role played by the COX/PG axis in parasites during the pathogenic processes and life cycles of these organisms. Parasites have the necessary machinery to synthesize eicosanoids; however, few reports document cyclooxygenase activity in protozoa. In this context, the only description of both a COX-like activity and the role of prostaglandins in the pathogenicity process was reported in the protozoan parasite *E. histolytica* [5,6]. In the case of *Leishmania*, it was documented that it can metabolize AA to prostaglandins using cyclooxygenase (COX) activity [7]. In this context, it has just been published that other parasites could also have this activity [15]. In this work, it is now demonstrated that a gp63 mutant protein from *L. mexicana* lacking the catalytic active site of the protease is unable to process arachidonic acid, the substrate of COX activity. In addition, by bioinformatics analysis, we report that medically important parasites possess hypothetical proteins orthologous to *L. mexicana* gp63. This is the case for *E. dispar*, *E. invadens* and *N. fowleri*, whereas a putative orthologous protein was identified in *A. castellanii*. In contrast, in *T. cruzi* and *E. histolytica*, Tcgp63-I and EhMSP-2 respectively, were identified as orthologous proteins with identity to *L. mexicana* gp63. *T. cruzi* was shown to possess ten or more gp63 or gp63-like genes, as in most

*Leishmania* spp. Two of these groups, Tcgp63-I and -II, are present as high-copy number genes. Tcgp63-I encodes surface proteins attached to the membrane through a GPI anchor, with a molecular weight of ~78 kDa, which are differentially expressed during the life cycle of the parasite. In contrast, the Tcgp63-II group is barely expressed. Both Tcgp63 and gp63 from *Leishmania* spp have the consensus sequence for the zinc-binding site, a region associated with metalloprotease activity (Figure 3 A). Likewise, the most critical residues for the catalytic activity, both His and Glu in the HEXXH motif, are completely conserved in the Tcgp63-I and Tcgp63 II groups [11,28,29]. To identify which of the proteins (Tcgp63-I and Tcgp63 II) was the orthologous protein, blast analysis was performed using Tcgp63-I and Tcgp63-II as target sequences and the *L. mexicana* gp63 as the query sequence. The result showed that the identified protein (XP\_817808.1, Table 1) had 76.94% to 78.4% identity with proteins belonging to the "a" and "b" members, respectively, of the Tcgp63-I group (data not shown). A possible involvement of the orthologous enzyme gp63 in the life cycle of this trypanosomatid should be investigated in future work, with particular emphasis on the AA binding site, which was theoretically established in *T. cruzi* by hydrogen bonding with TYR379 and ARG416 (Table 4). This analysis may be essential to correlate COX activity with the life cycle of this parasite. In the case of *E. histolytica*, the genome has been documented to contain two homologs of the leishmanolysin metalloprotease gene, *E. histolytica* MSP-1 and MSP-2. The nomenclature of this leishmanolysin corresponds to EhMSP-1 and EhMSP-2 [14] (NCBI GeneID: numbers 3409717 and 3406949, respectively); while the commensal amoeba *E. dispar* lost EhMSP-1. By searching for the products of these genes and comparing them with the orthologous sequence identified in the study (XP\_652632.1, Table 1), we confirm that the orthologous protein corresponds to EhMSP-2. Recent studies have shown that EhMSP-1 is involved in the regulation of amoeba adhesion, with additional effects on cell motility, disruption of cell monolayer, and phagocytosis [14]. More recently, the underlying mechanisms of adhesion and altered motility in EhMSP-1 deficient trophozoites have been shown to be the basis for identifying critical kinases and phosphatases for the control of amoebic invasiveness [30]. However, in the case of EhMSP-2, studies have not addressed a role of EhMSP-2 during these processes. Previous work by our group showed the presence in soluble fractions of *E. histolytica* trophozoites of proteins antigenically related to mouse COX, identified in Western blot and in immunofluorescence assays, using a commercial anti-mouse COX antibody. Although the existence of alpha-actinin-associated cyclooxygenase activity in *E. histolytica* has been previously reported [5], it is very likely that this parasite possesses more than one protein with this activity, since in this work we are demonstrating that EhMSP2 can bind arachidonic acid. Therefore, *E. histolytica* could potentially possess various COX-like activities. Regarding the hypothetical orthologous proteins identified in the *E. dispar*, *E. invadens*, and *N. fowleri* parasites, the analyses in predictive functional platforms, as well as the analyses in mRNA repositories, revealed that the identified proteins correspond to surface proteins with metalloendopeptidase activity, where mRNA levels were detected in the case of *E. invadens* and *N. fowleri*. Furthermore, in the case of the encystation process of *E. invadens*, in the immunofluorescence analyses, the presence of crossed antigenicity was determined using the commercial anti-gp63 antibody of *L. major*. Furthermore, biochemical analyses with exogenous AA (20 mM) revealed the presence of COX activity in *E. invadens* and *E. dispar* (Figure 8A). When encystation kinetics were performed, a maximum peak of activity was observed 48 h after the onset of encystation. In the case of *E. histolytica*, the presence of this activity was confirmed, as previously documented (Hernández-Ramírez et al., 2023). Recently the genome sequence of *N. fowleri* was purified using Oxford Nanopore Technology (ONT). This method assembled and polished the long reads, enabling the conservation of a high-quality genome [31]. In this context, the sequence of the protein, identified in this study as an orthologous protein of *L. mexicana* gp63 and whose accession number corresponded to KAF0981298.1, became hypothetical in the sequence genome improvement process of this parasite. In the case of this gp63-type protease, it would be necessary to define whether it participates during the invasion process, in the encystation process, or both functions. We are currently cloning the gene corresponding to the hypothetical protein (KAF0981298.1, Table 1) to deepen the knowledge of this orthologous protein in the biology of this free-living amoeba. Therefore, we can speculate that the parasitic protozoan species *E. dispar*, *E.*

*invadens*, and *N. fowleri* have a gp63-like, apparently differing from those identified in *T. cruzi* and *A. castellanii*. Concerning *A. castellanii*, the putative orthologue protein leishmanolysin was identified with accession number XP\_004337275 (Table 1) [32]. In this context, Gene Ontology Term (GOTerm) analysis suggests that this protein has the function of a zinc-binding metalloendopeptidase. However, analysis of RNA repositories has not yet revealed the presence of mRNA for this putative leishmanolysin protein. In this context, we recently reported both the presence of COX activity in soluble fractions of *A. castellanii* trophozoites, and a cross-reaction with the D12 monoclonal antibody that recognizes *L. mexicana* gp63[15]. In addition to this evidence, it is important to highlight that when reviewing both the prediction function data and the multiple alignment analyses, it was confirmed that the analyzed proteins have zinc-binding sites, as is the case with Tcgp63 protein II (XP\_817808.1, Table 1) and EhMSP-2 (XP\_652632.1, Table 1), as well as in the case of the putative leishmanolysin protein from *A. castellanii*. The potential binding site for this ion was also identified in the hypothetical orthologous proteins present in *E. invadens*, *E. dispar*, and *N. fowleri*. On the other hand, the domain analysis and the predictive functional analysis revealed that all examined proteins are classified into the M8 peptidase family. This implication needs to be validated experimentally, focusing primarily on the hypothetical orthologous proteins, because no information is available. In the case of the AA binding site, the species infecting humans were found to have similar binding sites (HIS206 and HIS267 and GLU207 for *E. histolytica* and *E. dispar*). In the case of *E. invadens*, the binding site was established through hydrophobic interactions, suggesting the relevance of the environment in which these amoebae parasitize. In the genus *Entamoeba*'s case, the results could suggest an involvement of the orthologue proteins in the life cycle of these parasites, especially in the encystation process (Figure 8D and 8E). In this regard, a previous report published by Siddiqui et al., [33] the non-steroidal anti-inflammatory drug (NSAID), sodium diclofenac, which targets the activity of COX, was shown to affect the growth but not the viability of *A. castellanii*. It is relevant to notice that NSAIDs (sodium diclofenac and indomethacin) abolished encystation in *A. castellanii*. Therefore, the authors propose that cyclooxygenases and prostaglandins of parasitic origin play an essential role in the biology of *Acanthamoeba*. However, COX activity has been reported for  $\alpha$ -actinin of *E. histolytica*, whose sequence lacks domains and residues necessary for COX activity. Among these residues, we can mention the presence, in the COX-like activity of *L. mexicana*, of the proton-accepting histidine at position 193, the metal-binding histidine at position 374, and tyrosine at position 371 within the active site [7]. In the case of the gp63 sequence, the multiple alignment allowed us to identify the presence of a glutamic acid and three metal-binding histidine (zinc) residues that could interact with tyrosine residues at positions 353 or 354 that are close to the active site (Figure 3A *L. mexicana*). The gp63 is a zinc-dependent metallopeptidase anchored to the plasma membrane by a glycosylphosphatidylinositol (GPI) tail, although hydrophilic and secreted isoforms have also been described. It belongs to the enzyme class EC 3.4.24.36 (MA clan, M8 endopeptidase family) and shares several similarities with mammalian matrix metallopeptidases [34]. In *Leishmania* spp, the functions described for this protein include various cellular processes ([35]. Recent findings ([7,15]) have shown that gp63 from *L. mexicana* can metabolize AA, indicating the role of gp63 as a multifunctional protein. In *E. dispar*, *E. invadens*, and *N. fowleri*, the description of proteins orthologous to gp63 of *L. mexicana* is new, but not in *E. histolytica* and *T. cruzi* since these proteins have already been identified as leishmanolysins; however, the role of these proteins in the metabolism of AA has not yet been described. A putative leishmanolysin protein has already been described in *A. castellanii* [36] and there is also a report indicating the possible presence of COX activity [33]. Considering that the genes encoding gp63 are organized in tandem, it will be necessary for future research to show whether COX-like activity would arise from all these encoded proteins. Recently published work compared active sites residues and protein sequences from gp63 with COX activity and prostaglandin F2 $\alpha$  synthase (PGFS) in *Leishmania* species and showed an alignment and phylogenetic analysis of GP63 and PGFS indicated notable similarity and homology between the Old and New World *Leishmania* spp [37]. Additional results revealed that PGFS enzymes increased during parasitic differentiation in various *Leishmania* species; and that the gp63 enzyme with COX-like activity reduces during *L. braziliensis* and *L. infantum* promastigotes differentiation, but no differences



were observed in *L. amazonensis* [37]. Finally, the results obtained with the molecular docking analyses suggest that proteins orthologous to gp63 could be targets for studies to develop drugs whose central purpose would be to control and/or interrupt the transmission cycle in the infection of the various parasites analyzed that are of clinical importance in this study.

## 5. Conclusions

COX activity was determined in the presence of exogenous AA in extracts of *E. dispar* trophozoites and in both *E. invadens* trophozoites and cysts. Likewise, after *in silico* analyses performed on gp63-like protein sequences in various parasites of clinical importance, such as *T. cruzi*, *E. histolytica*, *E. dispar*, *E. invadens*, *A. castellanii* and *N. fowleri* found these proteins to be orthologous to gp63 of *L. mexicana*. Therefore, we suspect these are likely the proteins responsible for COX-like activity in these parasites due to the presence of a theoretical sequence pointing to a probable AA union site. Performing site-directed mutations in these theoretical sequences will be vital to validating our hypothesis.

**Author Contributions:** CN.O.ceptualization, V.-I.H.-R., P.T.-R. and A.-S.M.-M. Formal Analysis: L.-A.C.-J. Funding acquisition: P.T.-R. Investigation: N.O., M.-A.M.-C., SVL. Methodology: V.-I.H.-R., A.-S.M.-M., N.O., C.O.-T. Project administration: P.T.-R. Resources: P.T.-R., A.-S.M.-M., L.-A.C.-J. Supervision: P.T.-R., V.-I.H.-R. Validation & Visualization: V.-I.H.-R., A.-S.M.-M., N.O., M.-A.M.-C., C.O.-T., L.S.-V., L.-A.C.-J., P.T.-R. Writing -original draft & review & editing: P.T.-R., V.-I.H.-R. All authors have read and agreed to the published version of the manuscript.

**Funding:** This research was funded by CONAHCYT (Basic Science), grant number A1-S-15223

**Acknowledgments:** We thank Angélica Leticia Serrano-Ahumada, ascribed to the Bioinformatics, Experimental Medicine Research Unit, Faculty of Medicine, UNAM, for her valuable participation in the processing and presentation of immunofluorescence images; Jessica Márquez-Dueñas for her secretarial assistance; and José Daniel Morales-Mora for his technical assistance in the processing of the materials used in the COX activity determination assays.

**Conflicts of Interest:** The authors declare no conflicts of interest.

## References

1. Bosetti, F. Arachidonic Acid Metabolism in Brain Physiology and Pathology: Lessons from Genetically Altered Mouse Models. *J Neurochem* 2007, 102, 577–586, doi:10.1111/j.1471-4159.2007.04558.x.
2. Balsinde, J.; Winstead, M. V.; Dennis, E.A. Phospholipase A<sub>2</sub> Regulation of Arachidonic Acid Mobilization. *FEBS Lett* 2002, 531, 2–6, doi:10.1016/S0014-5793(02)03413-0.
3. Kudo, I.; Murakami, M. Prostaglandin E Synthase, a Terminal Enzyme for Prostaglandin E<sub>2</sub> Biosynthesis. *BMB Rep* 2005, 38, 633–638, doi:10.5483/BMBRep.2005.38.6.633.
4. Rouzer, C.A.; Marnett, L.J. Cyclooxygenases: Structural and Functional Insights. *J Lipid Res* 2009, 50, S29–S34, doi:10.1194/jlr.R800042-JLR200.
5. Dey, I.; Keller, K.; Belley, A.; Chadee, K. Identification and Characterization of a Cyclooxygenase-like Enzyme from *Entamoeba Histolytica*. *Proceedings of the National Academy of Sciences* 2003, 100, 13561–13566, doi:10.1073/pnas.1835863100.
6. Lejeune, M.; Moreau, F.; Chadee, K. Prostaglandin E<sub>2</sub> Produced by *Entamoeba Histolytica* Signals via EP4 Receptor and Alters Claudin-4 to Increase Ion Permeability of Tight Junctions. *Am J Pathol* 2011, 179, 807–818, doi:10.1016/j.ajpath.2011.05.001.
7. Estrada-Figueroa, L.A.; Díaz-Gandarilla, J.A.; Hernández-Ramírez, V.I.; Arrieta-González, M.M.; Osorio-Trujillo, C.; Rosales-Encina, J.L.; Toledo-Leyva, A.; Talamás-Rohana, P. Leishmania Mexicana Gp63 Is the Enzyme Responsible for Cyclooxygenase (COX) Activity in This Parasitic Protozoa. *Biochimie* 2018, 151, 73–84, doi:10.1016/j.biochi.2018.05.016.
8. Ramamoorthy, R.; Donelson, J.E.; Paetz, K.E.; Maybodi, M.; Roberts, S.C.; Wilson, M.E. Three Distinct RNAs for the Surface Protease Gp63 Are Differentially Expressed during Development of Leishmania Donovanii Chagasi Promastigotes to an Infectious Form. *Journal of Biological Chemistry* 1992, 267, 1888–1895, doi:10.1016/S0021-9258(18)46030-9.
9. Rawlings, N.D.; Barrett, A.J. [13] Evolutionary Families of Metallopeptidases. In; 1995; pp. 183–228.

10. El-Sayed, N.M.A.; Donelson, J.E. African Trypanosomes Have Differentially Expressed Genes Encoding Homologues of the Leishmania GP63 Surface Protease. *Journal of Biological Chemistry* 1997, 272, 26742–26748, doi:10.1074/jbc.272.42.26742.
11. Grandgenett, P.M.; Coughlin, B.C.; Kirchhoff, L.V.; Donelson, J.E. Differential Expression of GP63 Genes in Trypanosoma Cruzi. *Mol Biochem Parasitol* 2000, 110, 409–415, doi:10.1016/S0166-6851(00)00275-9.
12. LaCount, D.J.; Gruszyński, A.E.; Grandgenett, P.M.; Bangs, J.D.; Donelson, J.E. Expression and Function of the Trypanosoma Brucei Major Surface Protease (GP63) Genes. *Journal of Biological Chemistry* 2003, 278, 24658–24664, doi:10.1074/jbc.M301451200.
13. Biller, L.; Davis, P.H.; Tillack, M.; Matthiesen, J.; Lotter, H.; Stanley, S.L.; Tannich, E.; Bruchhaus, I. Differences in the Transcriptome Signatures of Two Genetically Related Entamoeba Histolytica Cell Lines Derived from the Same Isolate with Different Pathogenic Properties. *BMC Genomics* 2010, 11, 63, doi:10.1186/1471-2164-11-63.
14. Teixeira, J.E.; Sateriale, A.; Bessoff, K.E.; Huston, C.D. Control of Entamoeba Histolytica Adherence Involves Metallosurface Protease 1, an M8 Family Surface Metalloprotease with Homology to Leishmanolysin. *Infect Immun* 2012, 80, 2165–2176, doi:10.1128/IAI.06389-11.
15. Hernández-Ramírez, V.I.; Estrada-Figueroa, L.A.; Medina, Y.; Lizarazo-Taborda, M.R.; Toledo-Leyva, A.; Osorio-Trujillo, C.; Morales-Mora, D.; Talamás-Rohana, P. A Monoclonal Antibody against a Leishmania Mexicana COX-like Enzymatic Activity Also Recognizes Similar Proteins in Different Protozoa of Clinical Importance. *Parasitol Res* 2023, 122, 479–492, doi:10.1007/s00436-022-07746-7.
16. Diamond, L.S.; Harlow, D.R.; Cunnick, C.C. A New Medium for the Axenic Cultivation of Entamoeba Histolytica and Other Entamoeba. *Trans R Soc Trop Med Hyg* 1978, 72, 431–432, doi:10.1016/0035-9203(78)90144-X.
17. Altschul, S.F.; Gish, W.; Miller, W.; Myers, E.W.; Lipman, D.J. Basic Local Alignment Search Tool. *J Mol Biol* 1990, 215, 403–410, doi:10.1016/S0022-2836(05)80360-2.
18. Madeira, F.; Park, Y. mi; Lee, J.; Buso, N.; Gur, T.; Madhusoodanan, N.; Basutkar, P.; Tivey, A.R.N.; Potter, S.C.; Finn, R.D.; et al. The EMBL-EBI Search and Sequence Analysis Tools APIs in 2019. *Nucleic Acids Res* 2019, 47, W636–W641, doi:10.1093/nar/gkz268.
19. Mistry, J.; Chuguransky, S.; Williams, L.; Qureshi, M.; Salazar, G.A.; Sonnhammer, E.L.L.; Tosatto, S.C.E.; Paladin, L.; Raj, S.; Richardson, L.J.; et al. Pfam: The Protein Families Database in 2021. *Nucleic Acids Res* 2021, 49, D412–D419, doi:10.1093/nar/gkaa913.
20. Kumar, S.; Stecher, G.; Li, M.; Knyaz, C.; Tamura, K. MEGA X: Molecular Evolutionary Genetics Analysis across Computing Platforms. *Mol Biol Evol* 2018, 35, 1547–1549, doi:10.1093/molbev/msy096.
21. Biasini, M.; Bienert, S.; Waterhouse, A.; Arnold, K.; Studer, G.; Schmidt, T.; Kiefer, F.; Cassarino, T.G.; Bertoni, M.; Bordoli, L.; et al. SWISS-MODEL: Modelling Protein Tertiary and Quaternary Structure Using Evolutionary Information. *Nucleic Acids Res* 2014, 42, W252–W258, doi:10.1093/nar/gku340.
22. Sippl, M.J.; Wiederstein, M. A Note on Difficult Structure Alignment Problems. *Bioinformatics* 2008, 24, 426–427, doi:10.1093/bioinformatics/btm622.
23. Mercado-Camargo, J.; Cervantes-Ceballos, L.; Vivas-Reyes, R.; Pedretti, A.; Serrano-García, M.L.; Gómez-Estrada, H. Homology Modeling of Leishmanolysin (Gp63) from *Leishmania Panamensis* and Molecular Docking of Flavonoids. *ACS Omega* 2020, 5, 14741–14749, doi:10.1021/acsomega.0c01584.
24. Pettersen, E.F.; Goddard, T.D.; Huang, C.C.; Couch, G.S.; Greenblatt, D.M.; Meng, E.C.; Ferrin, T.E. UCSF Chimera—A Visualization System for Exploratory Research and Analysis. *J Comput Chem* 2004, 25, 1605–1612, doi:10.1002/jcc.20084.
25. Yao, C.; Donelson, J.E.; Wilson, M.E. The Major Surface Protease (MSP or GP63) of Leishmania Sp. Biosynthesis, Regulation of Expression, and Function. *Mol Biochem Parasitol* 2003, 132, 1–16, doi:10.1016/S0166-6851(03)00211-1.
26. Wagh, P.K.; Peace, B.E.; Waltz, S.E. Met-Related Receptor Tyrosine Kinase Ron in Tumor Growth and Metastasis. In: 2008; pp. 1–33.
27. Yang, H.; Rothenberger, E.; Zhao, T.; Fan, W.; Kelly, A.; Attaya, A.; Fan, D.; Panigrahy, D.; Deng, J. Regulation of Inflammation in Cancer by Dietary Eicosanoids. *Pharmacol Ther* 2023, 248, 108455, doi:10.1016/j.pharmthera.2023.108455.
28. Cuevas, I.C.; Cazzulo, J.J.; Sánchez, D.O. Gp63 Homologues in *Trypanosoma Cruzi*: Surface Antigens with Metalloprotease Activity and a Possible Role in Host Cell Infection. *Infect Immun* 2003, 71, 5739–5749, doi:10.1128/IAI.71.10.5739-5749.2003.

29. Kulkarni, M.M.; Olson, C.L.; Engman, D.M.; McGwire, B.S. *Trypanosoma Cruzi* GP63 Proteins Undergo Stage-Specific Differential Posttranslational Modification and Are Important for Host Cell Infection. *Infect Immun* 2009, 77, 2193–2200, doi:10.1128/IAI.01542-08.
30. Hasan, M.M.; Teixeira, J.E.; Lam, Y.-W.; Huston, C.D. Coactosin Phosphorylation Controls Entamoeba Histolytica Cell Membrane Protrusions and Cell Motility. *mBio* 2020, 11, doi:10.1128/mBio.00660-20.
31. Liechti, N.; Schürch, N.; Bruggmann, R.; Wittwer, M. Nanopore Sequencing Improves the Draft Genome of the Human Pathogenic Amoeba Naegleria Fowleri. *Sci Rep* 2019, 9, 16040, doi:10.1038/s41598-019-52572-0.
32. Ramírez Verónica Ivonne, H.; Matus-Meza, A.-S.; Norma, O.; Castro Marco Antonio, M.; Trujillo Carlos, O.; Lizbeth, S.-V.; Luis Alejandro, C.-J.; Talamás-Rohana, P. *COX-like Activity in Parasites of Clinical Importance. Identification of Proteins Orthologous to Gp63 of Leishmania Mexicana and Exploration of Binding Sites with the Araquidonic Acid*;
33. Siddiqui, R.; Lakhundi, S.; Iqbal, J.; Khan, N.A. Effect of Non-Steroidal Anti-Inflammatory Drugs on Biological Properties of Acanthamoeba Castellani Belonging to the T4 Genotype. *Exp Parasitol* 2016, 168, 45–50, doi:10.1016/j.exppara.2016.06.011.
34. Etges, R.; Bouvier, J.; Bordier, C. The Major Surface Protein of Leishmania Promastigotes Is Anchored in the Membrane by a Myristic Acid-Labeled Phospholipid. *EMBO J* 1986, 5, 597–601, doi:10.1002/j.1460-2075.1986.tb04252.x.
35. d'Avila-Levy, C.M.; Altoé, E.C.F.; Uehara, L.A.; Branquinha, M.H.; Santos, A.L.S. GP63 Function in the Interaction of Trypanosomatids with the Invertebrate Host: Facts and Prospects. In; 2014; pp. 253–270.
36. Clarke, M.; Lohan, A.J.; Liu, B.; Lagkouvardos, I.; Roy, S.; Zafar, N.; Bertelli, C.; Schilde, C.; Kianianmomeni, A.; Bürglin, T.R.; et al. Genome of Acanthamoeba Castellani Highlights Extensive Lateral Gene Transfer and Early Evolution of Tyrosine Kinase Signaling. *Genome Biol* 2013, 14, R11, doi:10.1186/gb-2013-14-2-r11.
37. Andrade, Y.M.F. de S.; Castro, M.V. de; Tavares, V. de S.; Souza, R. da S.O.; Faccioli, L.H.; Lima, J.B.; Sorgi, C.A.; Borges, V.M.; Araújo-Santos, T. Polyunsaturated Fatty Acids Alter the Formation of Lipid Droplets and Eicosanoid Production in Leishmania Promastigotes. *Mem Inst Oswaldo Cruz* 2023, 118, doi:10.1590/0074-02760220160.

**Disclaimer/Publisher's Note:** The statements, opinions and data contained in all publications are solely those of the individual author(s) and contributor(s) and not of MDPI and/or the editor(s). MDPI and/or the editor(s) disclaim responsibility for any injury to people or property resulting from any ideas, methods, instructions or products referred to in the content.